ICSV14
Cairns • Australia
9-12 July, 2007
14th International Congress on Sound & Vibration

ROBUST FEEDBACK DISTURBANCE REJECTION FOR SOUND-STRUCTURE INTERACTION SYSTEMS USING OPTIMAL SENSOR – ACTUATOR LOCATION

Suwit Pulthasthan and Hemanshu Pota

School of Information Technology and Electrical Engineering,
University of New South Wales at Australian Defence Force Academy, ACT 2600, Australia
s.pulti@gmail.com

Abstract

This paper presents a practical method and novel work of robust disturbance rejection for sound-structure interaction systems using optimal sensor-actuator location. The applicability of this method is to systems with non-ideal boundary conditions as in the case of practical engineering applications. An experimental acoustic cavity with five walls of timber and a thin aluminium sheet fixed tightly on the cavity mouth is chosen in this paper as a good representation of general sound-structure interaction systems. The sheet is intentionally so fixed that it does not satisfy ideal boundary conditions. The existing methods for obtaining optimal sensor-actuator location using analytic models with ideal boundary conditions are of limited use for such problem with non-ideal boundary conditions. The optimal placement of actuator and sensor is obtained from novel criteria using energy based approach and model uncertainty. The optimal actuator-sensor location obtained is used to construct a robust feedback disturbance rejection using minimax LQG control design method. Practical aspects of the method of the robust feedback disturbance rejection using optimal sensor-actuator location are highlighted by experimental results of vibration and acoustic noise attenuation for arbitrary disturbance. The disturbance is experimentally set to enter the system via a spatial location different from the controller input like any practical applications of feedback disturbance rejections. Experimental demonstration of the novel methods presented in this paper attenuates structural vibration up to 17 dB.

1. INTRODUCTION

In this paper robust feedback disturbance rejection using optimal sensor-actuator location (OSAL) on a sound-structure interaction system (SSIS) has been investigated. The OSAL can enhance the robustness and the optimality of the feedback disturbance rejection. An experimental acoustic cavity pictured in Figure 1 is used as a good representation of general SSISs. The cavity with five walls of 10 *mm* thick timber has its mouth covered by a 1 *mm* thick aluminium sheet. The sheet is intentionally so fixed that it doesn't satisfy ideal boundary conditions. The work reported in this paper is done with a view to address the problem of practical SSISs with non-ideal boundary conditions, a norm in practical situation.

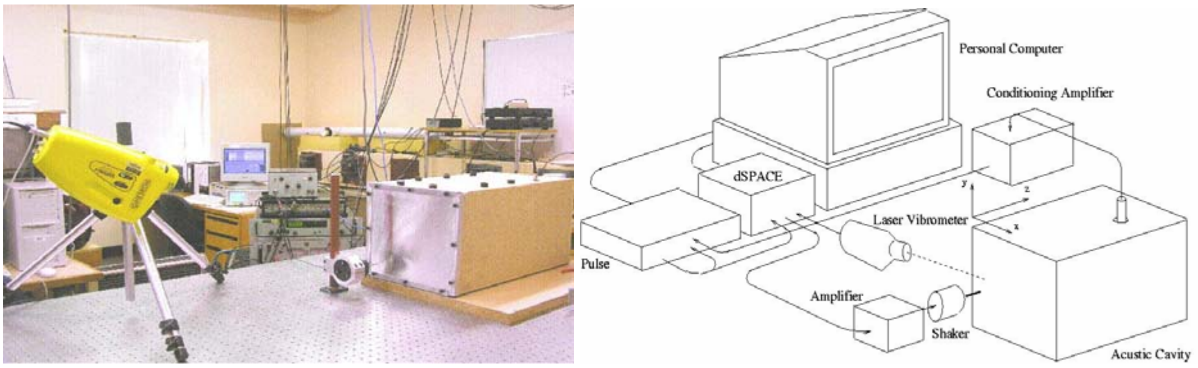

Figure 1. The experiment set-up.

Disturbance rejection can be achieved using feedback control [1]. The hindrance in the achievement of this goal is uncertainties in the model used to design a feedback control [2]. This practical problem leads to robust performance issues. In particular the models used for optimization and optimal control theory in modern control are mostly assumed to be ideal [3]. In practice, however, they suffer from the issue of robustness due to modelling errors [4], [5].

A large number of robustness problems in control system design have been researched [6]. Minimizing the norm with the consideration of model errors can increase the robustness significantly [7]. The performance is, however, often poor when optimizing for the worst case condition [7]. In the mixed design, which can achieve better performance in some situations, the performance measure is firstly optimized, then it is subjected to constraints to guarantee user determined stability robustness margins [8]. Minimax LQG control design method is developed to reduce the conservativeness of design [4].

The existing methods for obtaining OSAL using analytic models with ideal boundary conditions are of limited use for problems with non-ideal boundary conditions [9]. The present methods for OSAL can be systematically categorized as two main approaches [10]. One approach is based on integrating the problem of OSAL with a specific control design methodology, such as LQG, and treating the OSAL as extra design parameters. The other approach deals with the matter of OSAL independently from the control design problem. Once OSAL is obtained, a wide range of control design techniques can be employed for minimizing structural vibrations. Both approaches have been integrated in this paper.

The positioning method in this paper is developed from energy based approach and model uncertainty. The energy based approach is independent of the control design problem. It leads to controllability and observability gramian matrices [10], [11], [12], [13], [14]. These matrices present the qualitative controllability and observability of the system which depend on the positions of actuators and sensors. Furthermore, model uncertainty based on the uncertain system framework, which can enhance the robustness of feedback control [4], [15], [16], [17], is applied to an energy based approach. The model uncertainty concerns with a specific control design methodology. A stochastic model uncertainty is developed as an objective function and also used for minimax LQG control design method. This objective function integrates with other objective functions based on energy-based approach to find OSAL for practical SSISs. Practical aspects of the method are highlighted with experimental results of vibration and acoustic noise attenuation. The experiment is conducted such that the robust disturbance rejection works with disturbance entering the system through a different channel than the controller.

After introduction Section 2 describes the system and the experimental setup. Section 3 elaborates energy based approach which leads to the development of a new objective function for SSIS. In Section 4, relative criterion error (RCE) based on a new objective function is investigated. In Section 5, a frequency weighted uncertainty model of the uncertain system framework used to develop a novel criterion for OSAL is discussed. Further, a novel tool based on the uncertainty model is developed to ensure optimal and robust location of sensors and actuators when RCE method has multiple solutions in Section 6. Section 7 presents experimental vibration and acoustic noise attenuation of the feedback disturbance rejection.

2. SYSTEM DESCRIPTION

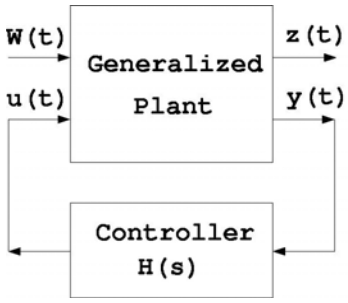

Figure 2. General feedback control system.

The cavity with the size of $(300\times300\times600)$ *mm* has the origin (0,0,0) at the bottom left corner of the aluminum sheet when one is facing it; *x*, *y*, and *z* axis is along the cavity width, height, and depth.

The cavity control problem is considered as a general feedback control system [2] presented in Figure 2. The signals *u*, *w*, *y*, and *z* are generally vector-valued function of time: *u* are controlled inputs, *w* is the disturbance vector, *y* contains all sensor outputs, and the *z* components represent the uncertainty output. Our control problem is single-input-single-output, hence *u*, *w*, *y*, and *z* are scalar. The control input *u* imposing on the sheet point-wise is applied by an electromachanic shaker (EMS). The output *y* is point-wise velocity of the vibrating sheet sensed by a laser-doppler-vibrometer (LDV). The air-pressure generated inside the cavity is measured by a microphone. System frequency responses from the EMS to the LDV and to the microphone are recorded by a multi-analyzer. The multi-analyzer also generates a swept sinusoidal disturbance signal from 10-300 Hz which is chosen in line with successful acoustic noise control experiments for reverberant environments with diverse methods [20], [21], [22].

The EMS and LDV implementation as actuator and sensor instead of piezoelectric transducers (PZT) is due to the relocation need during OSAL experimentation. PZT is intensively used in similar researches. The assumption of dynamics free of PZT from any effects of structure dynamics [10], [11] is not always valid. The EMS and LDV have this assumption as an inherent property.

3. SYSTEM ENERGY-BASED APPROACH

Energy-based approach for actuator and sensor positioning is based on system controllability and observability [23], which can be determined using many algorithms [7]. A useful approach to OSAL using system controllability and observability leads to a criterion on the eigenvalues of the controllability and observability gramian matrices. Both matrices are used to determine the controllability and observability properties qualitatively with less calculation difficulties [10], [11], [12], [13], [14]. The controllability gramian W_c and observability grammian W_o are defined as $W_c = \int_0^{T_f} e^{A\tau} BB^T e^{A^T\tau} d\tau$, and $W_o = \int_0^{\infty} e^{A^T\tau} C^T C e^{A\tau} d\tau$. Both W_c and W_o satisfy the Lyapunov equations, $AW_c + W_c A^T + BB^T = 0$, and $A^T W_o + W_o A + C^T C = 0$.

The Leleu et al. work [11] is applied to the OSAL problems. The gramian properties are developed for an object function (OF) *G*, $G = \dfrac{trace(W)\sqrt[2N]{\det(W)}}{\sigma(\lambda_i)}$, under the low dampings conditions and well separated eigenfrequencies [11].

W is either W_c for actuator locations or W_o for sensor positions. *N* is the system order. $\sigma(\lambda_i)$ is the standard deviation of the gramian eigenvalues λ_i. *OSAL is the position of max. G*. *G* is evaluated for different model techniques employed to the sheet. The evaluations present poor consistency of *G*. The uncertainty in the models can be a good reason. Hence, *G* and model uncertainty are integrated to develop a new OF in the next sections.

4. RELATIVE CRITERION ERROR

From physical point of view, OSAL for a flexible structure cannot be different for different models. In practice approximations apply to the true model due to the non-ideal boundary conditions, etc. It is observed that different models result in different OSAL. A particular model for the OSAL calculation and controller design should be selected such that those sensor-actuator location features are best captured. The features are most important in the optimization process.

A new OF, Relative Criterion Error (*RCE*), is developed based on the idea that at OSAL the identified model should be the closest fit with the experimental data compared to other actuator-sensor locations. In other words, that particular location is the best where the model uncertainty is the least. *G* obtained from OSAL should then provide numerical values with small difference if the models are fitted in different frequency ranges, and if these frequency ranges still contain the same vibration modes. To quantify the difference in numerical values of *G* for different identified models fitted in different frequency range, *RCE* is defined as:

$$RCE(L_a, L_s) = \max.\left|\frac{G_{10-300}(L_a, L_s) - G_{F-300}(L_a, L_s)}{G_{10-300}(L_a, L_s)}\right| \tag{1}$$

where L_a is actuator location, L_s is sensor location, $G_{10-300}(L_a, L_s)$ is either $G_c(L_a, L_s)$ for optimal actuator placement or $G_o(L_a, L_s)$ for optimal sensor placement derived from the identified model fitted in 10 - 300 Hz frequency range, and $G_{F-300}(L_a, L_s)$ is similar to $G_{10-300}(L_a, L_s)$ but with 10 Hz < $F \leq$ 90 Hz.

We note that for OSAL *RCE should be minimum*. ***Hence, OSAL = minimum*** $RCE(L_a, L_s)$. OSAL can be considered as the process of searching minimum *RCE*. Let us define RCE_C as *RCE* derived from G_C and RCE_O as *RCE* derived from G_O.

The numerical $RCE(L_a, L_s)$ values are calculated with the lower frequency range limit of $G_{F-300}(L_a, L_s)$ altered from 11 Hz to 90 Hz in steps of 1 Hz whereas the upper frequency range is fixed at 300 Hz. The models obtained from these ninety different frequency responses, with frequency range of 11 -, 12 -,…, 90 - 300 Hz, should gradually alter without sharp change. Maximum lower frequency limit is selected at 90 Hz. Since the first remarkable experimental natural frequency of the sheet from the measured frequency response appears around 90 Hz. This natural frequency can affect models which include this frequency. Although the first or lowest experimental natural frequency is approximately at 50 Hz, the associated amplitude is too small to affect models which include or do not include this frequency. Therefore, the $RCE(L_a, L_s)$ values obtained from the models based on these ninety frequency responses should smoothly change from one position to next position on the grid.

System identification [24] based on frequency responses from 196 collocated actuator-sensor positions along a coarse grid on the sheet is applied for RCE_C based on 10^{th} order model. The grid points are 20 *mm* apart. The reason for using 10^{th} order model is explained in Section 6. The obtained RCE_C values yield an interesting outcome. The very small RCE_C values concentrated in the area close to the origin corner at (0, 0, 0). The smallest RCE_C is at (30, 30) *mm* or the assumed optimal actuator position $\hat{L}_a$ = (30,30) *mm*.

5. UNCERTAINTY MODELLING

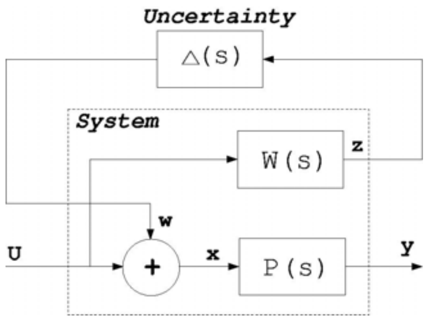

Figure 3. Uncertain system representation.

An uncertain system model is introduced in this section. The uncertainty is considered in approximating the measured frequency response data by a finite dimensional transfer function. The main uncertainty concerns with spillover dynamics. It is represented by frequency weighted multiplicative uncertainty as shown in Figure 3.

Figure 3 shows $\frac{Y(s)}{U(s)} = \tilde{P}(s) = P(s)[1 + \Delta(s)W(s)]$, where $\tilde{P}(s)$ and $P(s)$ are the true and identified model transfer function from the EMS to the LDV, respectively. Here *W(s)* is a suitable frequency weighting transfer function. It is the key function in designing a specific optimal controller. The uncertainty block can be any dynamical system satisfying a general uncertainty constraint [4], [25] which is particularly satisfied by the uncertainty block $\Delta(s)$, an uncertain transfer function. It is chosen such that $|\Delta(j\omega)| \leq 1 \,\forall\, \omega$.

From $\frac{Y(s)}{U(s)} = \tilde{P}(s) = P(s)[1 + \Delta(s)W(s)]$, it yields $\frac{\tilde{P}(s) - P(s)}{P(s)} = = \Delta(s)W(s)$. To restrict $|\Delta(j\omega)| \leq 1 \,\forall\, \omega$, the weighting function needs to be

$$\left|\frac{\tilde{P}(j\omega) - P(j\omega)}{P(j\omega)}\right| = |W(j\omega)| \,\forall\, \omega . \tag{2}$$

The bound (2) is an inequality bound on the *W(s)* magnitude. Many functions can satisfy the bound. In this paper the left-hand-side function of the bound (2) is computed in the interested frequency range from the experimental measurement and the identified system model. From these functions, a magnitude envelope is constructed and finally matched by a transfer function obtained using the Yule-Walker method in [26], [27]. Next, the uncertainty model is developed for a novel criterion for OSAL.

6. CRITERION OF UNCERTAINTY BOUND ERROR

Since *RCE* is based on energy approach and model errors, an additional OF based on *RCE* is developed from (2) as Criterion of Uncertainty Bound Error (*CUBE*) to support *RCE* in case of multiple *RCE* solutions. *CUBE* represents the absolute value of difference between the relative error of the true and identified model, $\frac{\tilde{P}(j\omega)-P(j\omega)}{P(j\omega)}$, and the weighting function $W(j\omega)$ in any frequency range, see (2), as

$$CUBE(L_a, L_s) = \min 20\log \left\| \left| \frac{\tilde{P}_{L_a,L_s}(j\omega) - P_{L_a,L_s}(j\omega)}{P_{L_a,L_s}(j\omega)} \right| - \left| W_{L_a,L_s}(j\omega) \right| \right\|, \tag{3}$$

where $\omega = F \times 2\pi, \ldots, 300 \times 2\pi$ with 10 Hz < $F \le$ 90 Hz, $\tilde{P}_{L_A,l_S}(j\omega)$ is the measured transfer function from the actuator, EMS, at L_a position to the sensor, LDV, at L_s position, and $P_{L_a,L_s}(j\omega)$ is the identified model transfer function from the same actuator and sensor positions. $W_{L_a,L_s}(j\omega)$ is a stable frequency weighting function obtained using Yule-Walker method.

Minimum cost function (2), desirable for an associated optimal controller design, can be obtained where the identified model fits best with the experimental data or at OSAL. *CUBE* can support *RCE*, not to be the main OF for OSAL. It is based on the raw data of measured frequency responses, unlike *RCE* based on controllability and observability indices obtained from system (A,B,C,D) matrices. The matrices represent system dynamics in finite form.

The investigation of RCE_O and *CUBE* have been conducted on the grid points of 10 *mm* apart around the assumed optimal actuator position $\hat{L}_a$ = (30, 30) *mm* in Section 4. This time, RCE_O and *CUBE* are investigated using 7th – 12th order models due to the successful vibration control of the same cavity based on 7th order models in Pota et al. [28]. If the model order is lower than 7th order model, it leads to observation spillover that the identified model misses some physical vibration modes. If the model order is too high, it causes control spillover that vibration modes excluding from the identified model will be excited. Both types of spillover can destabilize the control system.

Table 1. RCE_O and *CUBE* and lower frequency range limit based on 10th order model.

y-axis (mm)	Values of RCE_O of collocated actuator and sensor position					Corresponding values of *CUBE* and RCE_O					Lower limit of frequency range				
60	0.25	0.60	0.32	0.29	0.31	103.26	71.30	85.39	120.37	111.55	90	34	24	86	73
50	0.19	0.51	0.29	0.24	0.30	97.89	61.48	82.08	13.96	118.60	55	33	26	73	78
40	0.09	0.31	0.30	0.30	0.35	82.39	59.10	68.74	91.43	136.63	61	25	27	25	79
30	0.09	0.19	0.38	2.72	0.53	68.63	54.59	56.92	164.85	96.72	62	74	27	55	22
20	0.07	0.46	0.84	1.20	1.74	61.81	67.48	70.84	72.22	88.96	65	37	36	36	35
x-axis	*20*	*30*	*40*	*50*	*60*	*20*	*30*	*40*	*50*	*60*	*20*	*30*	*40*	*50*	*60*

Table 1 shows that the best RCE_O and $CUBE$ combination with the associated lower frequency range limit of min $20\log\left|\frac{\tilde{P}_{L_a,L_s}(j\omega)-P_{L_a,L_s}(j\omega)}{P_{L_a,L_s}(j\omega)}\right| - \left|W_{L_a,L_s}(j\omega)\right|$, which is useful in the process of designing a controller, is surprisingly at the sensor position $\hat{L}_s$ = (20, 20) *mm*. At this OSAL the RCE_O value is 0.068 and the \$CUBE\$ value is 61.81 with the associated bottom frequency range limit of 65 Hz. This OSAL will be used to obtain an identified model for designing a minimax LQG controller.

7. EXPERIMENTAL RESULTS

Figure 4 shows the experimental control performance based on an identified model with the OSAL obtained from *RCE* and *CUBE* at $\hat{L}_a$ = (30, 30) *mm* and $\hat{L}_s$ = (20, 20) *mm*. This OSAL is selected instead of the collocated OSAL at $\hat{L}_a = \hat{L}_s$ = (30, 30) *mm* although OSAL is generally collocated. The LDV cannot exactly sense the vibration at the point imposed by the EMS when both EMS and LDV are on the same sheet side. The LDV can only sense the vibration closely around that point. The real collocated actuator and sensor positions provide the same coordinate of actuators and sensors. The actuators are on one side whereas the sensors on the other side which is impractical for the OSAL investigation for already built structures.

The experiment results up to 17 dB attenuation in vibration over the entire frequency range. The associated acoustic noise reduction inside the cavity is up to 10 dB without the explicit knowledge of the acoustic model. The result agrees with the reciprocity principle of a close relation between structural vibration and acoustic power radiation [18], [19]. The poor acoustic noise control at frequency 100 Hz is due to inefficient coupling of the structural vibration mode of the aluminium sheet with the acoustic mode at the frequency.

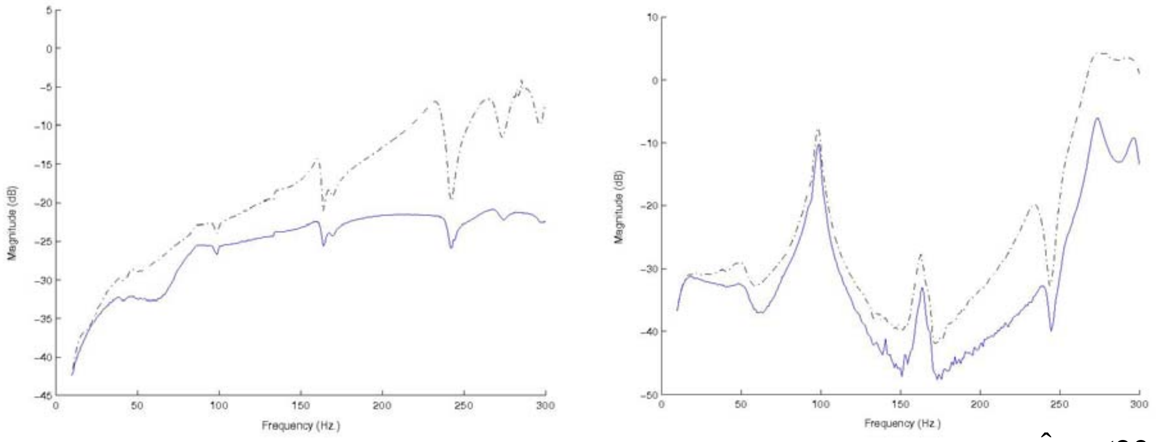

Figure 4. Experimental structural vibration (left) and acoustic noise (right) attenuation at $\hat{L}_a$ = (30, 30) *mm* and $\hat{L}_s$ = (20, 20) *mm* (dash line – Open Loop Response, solid line – Closed Loop Response)

8. CONCLUSIONS

A practical and novel method for OSAL for practical SSISs with non-ideal boundary condition is developed. The successful development is based on the integration of an uncertain system framework with energy based approach. The OSAL obtained using the new criteria improved the flexural vibration control dramatically. The associated acoustic noise inside the cavity is also attenuated effectively as suggested by the reciprocity principle.

REFERENCES

[1] G.F. Franklin, J.D. Powell, and A. Emami-Naeini, *Feedback control of dynamic systems*, Electrical and Computer Engineering, Control Engineering, Prentice Hall, 3rd edition, 2002.

[2] J.C. Doyle, B. Francis, and A. Tannenbaum, *Feedback control theory*, Macmillan, USA, 1992.

[3] P. Whittle, *Optimal Control: Basics and Beyond*, Wiley, New York, 1996.

[4] I.R. Petersen, V. Ugrinovskii, and A.V. Savkin, *Robust Control Design using $H\infty$ Methods*, Springer, New York, 2000.

[5] S.J. Elliott, *Signal Processing for Active Control*, Academic Press, London, UK, 2001.

[6] P. Dorato, R. Tempo, and G. Muscato, "Bibliography on robust control", *Automatica* **29(**1**):** 201-214, (1993).

[7] K. Zhou, J.C. Doyle, and K. Glover, *Robust and Optimal Control*, Prentice Hall, NJ, 1996.

[8] D.S. Bernstein, and W.M. Haddad, "LQG control with an $\mathrm{H}\infty$ performance bound: A Riccati equation approach", *IEEE Trans on AC* **34(**3**):** 293-305, March 1989.

[9] S.L. Padula, D.L. Palumbo, and R.K. Kincaid, "Optimal sensor/actuator locations for active structural acoustic control", *In 39th AIAA/ASME/ASCE/AHS/ASC Structures, Structural Dynamics, and Materials Conference*, volume 98-1865, Long Beach, California, 1998. IEE

[10] S.O.R. Moheimani, D. Halim, and A.J. Fleming, *Spatial Control of Vibration: Theory and Experiments*, World Scientific, New Jersey, 2003.

[11] S. Leleu, H. Abou-Kandil, and Y. Bonnasieux, "Piezoelectric actuators and sensors location for active control of flexible structures", *IEEE Transactions on Instrumentation and Measurement* **50**(6), 1577-1582, (2001).

[12] W.K. Gawronski, *Advanced Structural Dynamics and Active Control of Structures*, Springer, NY, 2004.

[13] W.K. Gawronski, *Actuator and sensor placement for structural testing and control*, Springer, NY, 1997.

[14] W.K. Gawronski, "Simultaneous placement of actuators and sensors", *Journal of Sound and Vibration* **228(**4**):** 915-922, (1999).

[15] H.R. Pota, S. Pulthasthan, and I.R. Petersen, "Robust control of an acoustic cavity", *Proceedings of the IEEE Conference on Control Applications*, Taipei, Taiwan, 2–4 September 2004, pp. 771-775.

[16] H.R. Pota, I.R. Petersen, and A.G. Kelkar, "Robust control of a 2D acoustic duct", ASME *Journal of Vibration and Acoustics* **125:** 374-383, (2003).

[17] H.R. Pota and A.G. Kelkar, "Modelling and control of acoustic ducts", *ASME Journal of Vibration and Acoustics* **123**(1)**:** 2-10, (2001).

[18] L. Cremer, M. Heckl, and E.E. Ungar, *Structure-Borne Sound*, Springer, Berlin, 1988.

[19] J.W.S.B. Rayleigh, "On the law of reciprocity in diffuse reflexion", Philosophical Magazine **49:** 324-325, (1900).

[20] C.R. Fuller and A.H. von Flotow, "Active control of sound and vibration", *IEEE Control Systems Magazine* **16**(6)**:** 9-19, (1995).

[21] S.M. Kim and M.J. Brennan, “A comparative study of feed forward control of harmonic and random sound transmission into an acoustic enclosure”, *Journal of Sound and Vibration* **226:** 549-571, (1999).

[22] S.J. Elliott, P.A. Nelson, I.M. Stothers, and C.C. Boucher “In-flight experiments on the control of propeller-induced cabin noise”, *Journal of Sound and Vibration* **140:** 219-38, (1990).

[23] T. Kailath, *Linear Systems*, Prentice Hall, Englewood Cliffs, New Jersey, 1980.

[24] T. McKelvey, H. Akçay, and L Ljung “Subspace-based multivariable system identification from frequency response data”, *IEEE Transactions on Automatic Control* **41**(7)**:** 960-979, (1996).

[25] V.A. Ugrinovskii and I.R. Petersen, “Time-averaged robust control of stochastic partially observed uncertain systems”, *Proceedings of the IEEE Conference on Decision and Control*, Tampa, Florida, December 1998.

[26] B. Friedlander and B. Porat, “The modified Yule-Walker method of ARMA spectral estimation”, *IEEE Transactions on Aerospace Electronic Systems* **20**(2)**:** 158-173, (1984).

[27] I.R. Petersen, H.R. Pota, and M.R.S. Jahromi, “System identification, uncertainty modelling and actuator placement in the robust control of an acoustic duct”, *In Conference on Information, Decision and Control*, Adelaide, Australia, February 2002.

[28] H.R. Pota, S. Pulthasthan, and I.R. Petersen, “Acoustic noise reduction in sound-structure interaction system”, *Proceedings of the 43rd IEEE Conference on Decision and Control*, Atlantis, Paradise Island, The Bahamas, 14–17 December 2004, pp. 5071-5076.